ACS Photonics

Article

pubs.acs.org/journal/apchd5

Enhanced Terahertz Emission from Schottky Junctions Using Plasmonic Nanostructures

Gopika K. P. Ramanandan,* Aurèle J. L. Adam, and Paul C. M. Planken

Optics Research Group, Department of Imaging Physics, Delft University of Technology, Lorentzweg 1, 2628 CJ, Delft, The Netherlands

Supporting Information

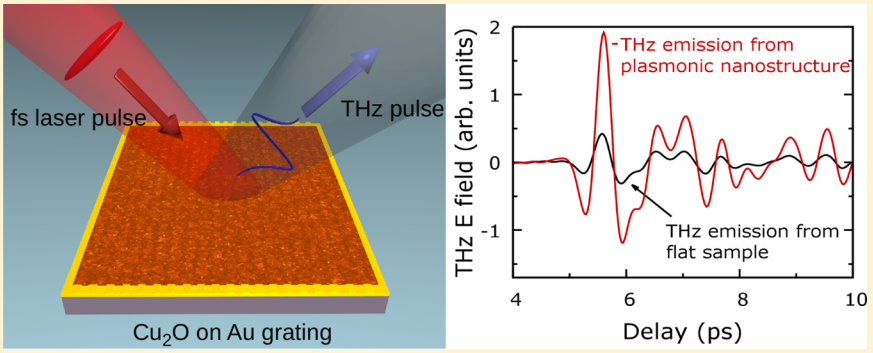

ABSTRACT: We present measurements of the enhanced emission of terahertz pulses after the optical excitation of grating-coupled near-IR surface plasmons at the interface of gold and cuprous oxide, using femtosecond laser pulses. Terahertz emission is the result of the acceleration of charge carriers optically excited in the Schottky depletion field of the metal/semiconductor interface. The enhancement is a direct consequence of the localized nature of the surface plasmon field, which is strongest near the nanostructured metal surface where the Schottky electric field is strongest too. Surface plasmon excitation is confirmed by reflection spectroscopy of gratings with different periods, by varying the azimuthal angle of the grating, and by calculations of the plasmon frequencies and fields. We observe a terahertz field enhancement factor of 5.8 when compared to the emission from a flat sample. This corresponds to a THz power-enhancement factor of 34. Our results show that for THz emission from these metal/semiconductor interfaces, it matters more where the pump light is absorbed than how much pump light is absorbed.

KEYWORDS: *terahertz generation, plasmonics, grating, Schottky junction, nanostructures, plasmonic enhancement*

Terahertz time-domain spectroscopy (THz-TDS) is an important technique to generate and detect THz radiation. In this technique the electric field of a quasi single-cycle THz light pulse is coherently detected, yielding both phase and amplitude information. It has many applications in science and technology, including imaging and spectroscopy.[1,2] There are quite a few methods to generate THz pulses, such as optical rectification[3,4] in crystals such as ZnTe, GaP, and GaSe, carrier acceleration in biased semiconductors such as GaAs,[5−7] and the photodember effect in materials like InAs.[8]

One of the earliest methods developed to generate THz radiation uses carrier acceleration in the static depletion electric field, or Schottky field, naturally formed at the interface between a metal and a doped semiconductor. These emitters come in the form of continuous layers[9,10] or, recently,[11,12] in the form of discontinuous periodic structures where, in addition to in-plane Schottky-field-induced THz emission, the lateral photodember effect plays a role. In general, however, Schottky interfaces are inefficient sources of THz radiation because the metal thin film, which is deposited on top of the semiconductor, partially blocks the incoming pump laser pulses and (in a reflection geometry) the generated THz pulses. Another important reason for the low efficiency is that the Schottky field strength decreases to zero at a certain depth in the semiconductor. If the optical absorption depth is considerably larger than this, many free carriers will be optically generated in a region of the semiconductor where there's no static electric field. These carriers do not contribute to the transient current and, thus, to the generation of THz light, strongly reducing efficiency. Recently, we demonstrated enhanced THz emission from these interfaces by reversing the order in which the metal and semiconductor layers are deposited, that is, by depositing a thin semiconductor film, such as cuprous oxide, (Cu_2O) on top of a metal substrate.[13] This increases the conversion efficiency because the semiconductor layer can now act like an absorbing antireflection coating on a metal, resulting in cavity-enhanced optical absorption.[14] In addition, by choosing a semiconductor layer thickness as close as possible to the Schottky depletion layer thickness, we can ensure that most of the pump-light gets absorbed in a region of the semiconductor where it matters for the generation of THz light. One reason why this development

Received: July 8, 2014
Published: October 30, 2014

is important is that thin metals and polycrystalline semiconductors such as Cu_2O can be deposited on many surfaces, such as curved mirrors. This makes them prime candidates for optical components with enhanced functionality, such as a mirror that acts as both the source of THz radiation and as the focusing element.

Despite this improvement, this situation is still far from ideal. The static Schottky electric field is strongest near the metal surface, whereas the electromagnetic boundary conditions for the pump pulse dictate that the pump field is weakest at the metal surface. In practice, therefore, most of the light is absorbed away from the metal in a region of the semiconductor where the Schottky field is relatively weak.

Here, by localizing the pump light at the metal/semiconductor interface, we show that it is possible to significantly enhance the emission of Schottky field THz emitters. Concentration of the pump light near the metal surface is achieved by excitation of optical surface plasmons on nanostructured gold/cuprous oxide interfaces. We show that this leads to increased optical absorption close to the metal surface where the Schottky electric field is also strongest. We find that, as a result, even a small increase in the optical absorption of less than 15% can give rise to an increase in the emitted THz power of a factor of 9. This shows that, for efficient THz emission, it matters more where the pump light is absorbed than how much pump light is absorbed. Our results may lead to new, integrated, plasmonic THz emitters.

A schematic diagram illustrating the idea of a nanostructured metal/semiconductor thin film THz emitter is shown in Figure 1(a). A gold nano grating is fabricated and covered with a thin

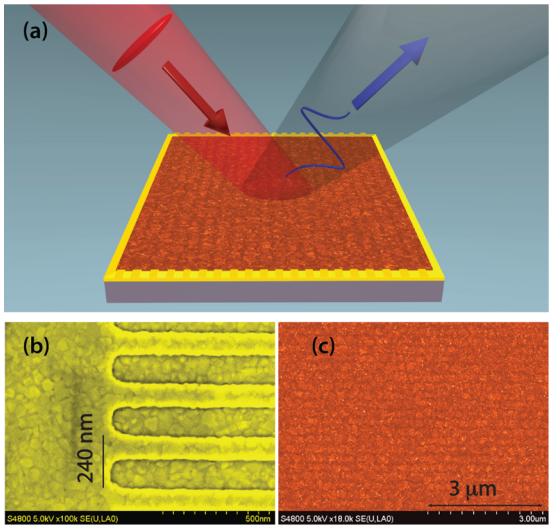

Figure 1. (a) Schematic diagram of the nanostructured Au/Cu_2O Schottky junction THz emitter. The pump laser pulses are incident on the sample, generating THz pulses. A nanograting is fabricated at the interface to facilitate the excitation of surface plasmons. (b, c) False color SEM image of the grating after the deposition of Au and Cu_2O, respectively.

Cu_2O film. Femtosecond laser pulses, centered around a wavelength of 800 nm, are incident on the Au/Cu_2O thin film THz emitter at an angle of incidence of 45°, and optically excite surface plasmons at the interface. The period of the grating required to excite plasmons at a particular wavelength can be found from the phase matching condition:[15]

$$k_{\mathrm{inc},x} + N\frac{2\pi}{\Lambda} = k_{\mathrm{sp}},\ N = \ldots, -1, 0, 1, \ldots \quad (1)$$

where $k_{\mathrm{inc},x}$ is the component of the incident wave vector parallel to the interface and $k_{\mathrm{sp}} = 2\pi/\lambda((\varepsilon_m\varepsilon_d)/(\varepsilon_m + \varepsilon_d))^{1/2}$ is the wave vector of the surface plasmon propagating along the interface, and ε_m and ε_d are the frequency-dependent dielectric permittivities of Au and Cu_2O respectively. $N2\pi/\Lambda$ is the additional wave vector k_g provided by the grating, N is the diffraction order, which is an integer that can have both positive and negative values, and Λ is the period of the grating.

For an angle of incidence of 45° on the air-dielectric interface, the grating period required to excite surface plasmons in the gold-cuprous oxide interface can be calculated from eq 1 to be ~240 nm. The electric permittivity values assumed are $\varepsilon_d = 5.39 + i0.28$, and $\varepsilon_m = -26.15 + i1.85$, at a wavelength of 800 nm.[13,16] A false color SEM image of an etched silicon grating after the evaporation of a thin film of gold is shown in Figure 1b. A false color SEM image of the sample surface after the deposition of the Cu_2O film on the Au grating is shown in Figure 1c. The details of the nanograting fabrication procedure are given in the Supporting Information.

An illustration of the experimental configuration showing the angle of incidence θ and the azimuthal angle ϕ between the plane of incidence of the pump beam and the grating vector $\vec{k}_g$ is shown in Figure 2. All our measurements were performed at

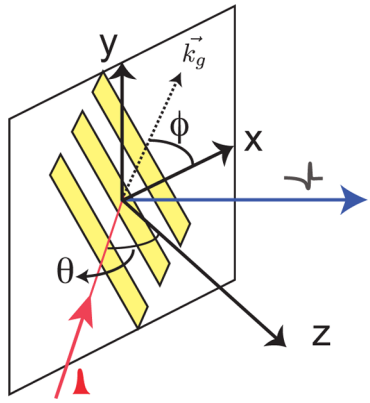

Figure 2. Illustration of the azimuthal angles ϕ and θ in the experimental configuration. The dashed line gives the direction of the grating wavevector.

an angle of incidence of 45°. The sample surface lies in the xy-plane and xz is the plane of incidence of the pump beam. To change the azimuthal angle, we rotate the grating about the z-axis.

Our goal is to prove that the excitation of grating-coupled surface plasmons enhances the emission of THz light from Cu_2O/Au interfaces. However, the Cu_2O layer constitutes a thick absorbing dielectric on top of a metal grating and it is not a foregone conclusion that surface plasmons can be found/measured in such a system. For this reason, the next section, "Reflection Spectroscopy", focuses on optical reflection measurements and on simple analytical calculations of the surface plasmon frequencies to establish the presence of visible/near-IR surface plasmons. Enhanced THz emission is demonstrated in the section "THz Emission" and further evidence for the role played by surface plasmons in the enhancement is presented in the section "Azimuthal Angle

dx.doi.org/10.1021/ph500251a | ACS Photonics 2014, 1, 1165−1172

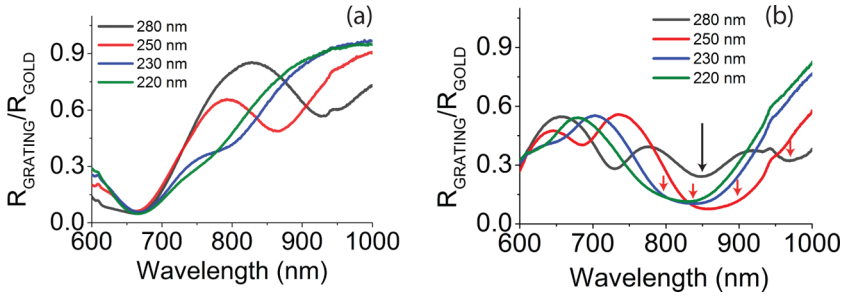

Figure 3. White-light reflection spectra of the nanostructured Au/Cu_2O samples with different grating periods, and with a Cu_2O thickness of (a) around 166 nm and (b) 232 nm. The light is incident at a polar angle of 45° and is p-polarized. The sample is oriented such that the azimuthal angle is 0°.

Dependence". Finally, we summarize our findings in the "Conclusion" section.

REFLECTION SPECTROSCOPY

In order to confirm that the pump laser light excites surface plasmons, we measured the reflection spectra of the nanostructured Au/Cu_2O samples having different grating periodicities, ranging from 220 to 300 nm. While fabricating the structures, the width of the grooves was kept constant at ∼140 nm, and only the width of the ridges was changed to change the grating period. To measure the white-light reflection spectra of these samples, we used a tungsten-halogen lamp as the light source, polarized in a direction parallel to the plane of incidence (p-polarized). The spectral intensity of the reflected light from the samples was measured using an "Ocean Optics" fiber-optic spectrometer and normalized to the reflection from a bare gold sample. The Cu_2O thickness is ∼166 nm in this case. The gratings were oriented at an azimuthal angle of 0° during the measurement. For p-polarized pump light, plasmons are excited when ϕ = 0° and are not excited when ϕ = 90°. The normalized reflection spectra of Cu_2O-covered gold nanogratings for different grating periodicities of 220, 230, 250, and 280 nm, are shown in Figure 3a. All the samples show a minimum in their reflection spectrum around a wavelength of 660 nm, which arises from destructive interference and coherent optical absorption of the waves reflected at the two interfaces of the Cu_2O thin film.[13,17] The low reflection implies that about 93% of the incident light is absorbed in the Cu_2O/Au sample at this wavelength, even without plasmon excitation. The reflection spectra also show minima whose position as a function of wavelength depends on the grating period. For example, a resonance is seen around a wavelength of 980 nm for the sample with a grating period of 280 nm. This resonance shifts to shorter wavelengths when the period is reduced. The dependence of this resonance wavelength on the grating period is indicative of plasmon excitation. For a period of 230 nm, the plasmon resonance is at 800 nm, corresponding to the wavelength of the pump laser used in THz generation experiments. In Figure S1 a of the Supporting Information, the reflection spectra of the samples when ϕ = 90° show that plasmon resonances are absent in this configuration, as expected. We emphasize that for these samples the Cu_2O thickness of 166 nm was chosen on purpose to move the effects of coherent optical absorption to a wavelength far removed from the plasmon excitation wavelength, allowing us to study the role that plasmons play in enhancing THz emission. However, for maximum THz emission, it seems plausible to let the plasmon excitation and coherent optical absorption coincide. For this reason we also fabricated samples where the Cu_2O thickness was 232 nm.[13,18] The reflection spectra from these samples, normalized by dividing them by the bare gold reflection spectrum, are shown in Figure 3b. It can be seen that the interference minima occur at a wavelength of ∼840 nm, which is not exactly at the pump laser wavelength of 800 nm, but close enough to significantly increase the absorption of the laser light compared to the absorption by the 166 nm thick layer. The dip in the reflection spectra caused by the destructive interference is marked by the black arrow. For a grating of period 300 nm, the plasmon resonance corresponding to N = −1 is visible around a wavelength of 975 nm. For a grating period close to 230 nm, the plasmon resonance merges with the reflection minimum near the laser excitation wavelength. As a guide to the eye, the approximate plasmon resonance positions are marked with red arrows. Another set of plasmon resonances can also be seen, in the spectral range 600−750 nm. For the grating of period 300 nm, this plasmon resonance occurs at a wavelength near 750 nm, and shifts to lower wavelengths as the period is decreased. These plasmon modes correspond to the case N = +1. Figure S1 b in the Supporting Information shows the reflection spectra of these samples at an azimuthal angle of 90°. Surface plasmon resonances are absent in the reflection spectra for this orientation.

The wavelengths at which the plasmon resonances are expected for the various grating periods can be calculated from the dispersion relation given by eq 1. We showed recently that when a Cu film deposited on a Au substrate is oxidized by heating the sample in the ambient atmosphere, interdiffusion of the metals result in the formation of a AuCu alloy at the interface between Au and the subsequently formed Cu_2O.[18] Refractive indices of the Cu_2O and AuCu thin films were measured using ellipsometry and these measured values were used to calculate the resonance wavelengths using eq 1. In Figure 4, we plot the wavelengths of the plasmon resonances which occur in the nanostructured Au/Cu_2O samples, as a function of the grating period Λ. In the wavelength range under consideration, two plasmon resonances are possible, corresponding to $N = \pm 1$, represented by the solid and dashed black lines, for N = −1 and N = 1 respectively. The scattered points in *red* show the plasmon resonance wavelengths measured from the set of samples with an oxide film thickness of 232 nm, and in *blue* are the measured resonances from the samples with an oxide film of thickness 166 nm. The plasmon resonance wavelengths corresponding to N = +1 are not shown for the samples with a Cu_2O thickness of 166 nm, since these plasmon resonances occur near to the deep interference minimum around 650 nm, and were difficult to determine. The plasmon

dx.doi.org/10.1021/ph500251a | ACS Photonics 2014, 1, 1165−1172

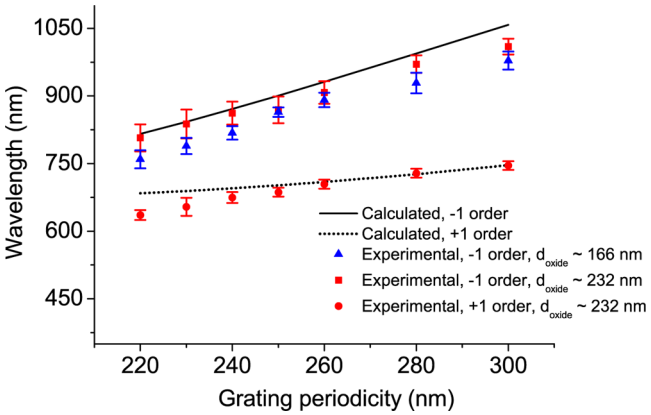

Figure 4. Vacuum wavelengths at which surface plasmon resonances occur at Au/Cu_2O interfaces are plotted as a function of the grating period. The dashed and the solid lines correspond to the expected plasmon resonance wavelengths from an *analytic* calculation, corresponding to $N = +1$ and $N = -1$, respectively. In the calculation, only a Au/Cu_2O interface is considered, and all the films are assumed to be infinitely thick. The blue triangles represent the *experimentally* determined resonance wavelengths for samples with a 166 nm thick Cu_2O layer on them. The red circles and squares represent the experimentally determined resonance wavelengths for samples with a 232 nm thick Cu_2O layer on them, and correspond to the $N = +1$ and $N = -1$ cases, respectively. For the sample of oxide thickness 232 nm, the plasmon resonance and the coherent optical absorption wavelengths coincide near to a sample period of 230 nm. The error bars are to indicate the uncertainty in determining the exact wavelengths of the plasmon resonances, from the reflection spectra measurements.

resonance wavelengths observed experimentally are close to the expected values. The differences between the measurements and calculations may be attributed to the error in the extracted refractive index values of the AuCu alloy and the Cu_2O thin film. It can also be seen from Figure 4 that the wavelengths at which plasmon resonances are experimentally observed match better with the analytically calculated resonance wavelengths for a Cu_2O thickness of 232 nm, than for the case of a thickness of 166 nm. This could be due to the fact that for the analytical calculation, the thickness of the Cu_2O layer is considered infinite. In other words, we ignore the effects of having a finite Cu_2O layer while determining the expected resonance wavelength for a particular grating period. A possible reason for this is that the extent of the plasmon field is larger than the thickness of the cuprous oxide thin film, resulting in a shift from the calculated plasmon resonance wavelength.

THZ EMISSION

Our experimental setup allows us to measure the electric field of the emitted THz pulses as a function of time and is described in more detail in the Supporting Information. An example of a measured THz electric field emitted by a nanostructured Au/Cu_2O sample having a grating period of 240 nm and an oxide thickness of around 166 nm, is shown in Figure 5. We find that the electric field amplitude emitted by the nanostructured sample is enhanced by a factor of around 5.8 compared to the field emitted by a flat, unstructured, sample. Note that this corresponds to a power enhancement factor of 34. The shape of the time-dependent electric field of the THz pulses emitted by the nanostructured sample is not different from that emitted by the flat sample, even though its amplitude is much larger. This means that within our measurement accuracy, and within

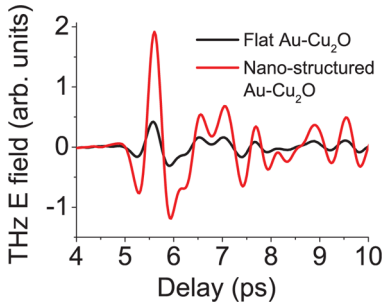

Figure 5. Time-dependent p-polarized electric field of the THz pulses emitted by the flat and the nanostructured Au−Cu_2O thin film interfaces at $\phi = 0°$. The nanostructured sample has a grating period of 240 nm at the Au−Cu_2O interface and an oxide thickness of around 166 nm.

the bandwidth of our detection setup, which is about 3.5 THz, the nanostructuring and plasmon excitation does not cause any changes to the spectrum of the emitted THz pulses.

The THz emission amplitude from the nanostructured Au/Cu_2O samples with 166 nm oxide thickness, as a function of grating period is shown in Figure 6a. We emphasize that, for this case, coherent optical absorption plays a negligible role. The electric field amplitude of the THz pulses emitted when $\phi = 0°$, the configuration that supports plasmon excitation is shown by the black points. The blue points show the field amplitude of the THz pulses emitted when $\phi = 90°$. For comparison, the THz emission from the flat Au/Cu_2O samples is also shown (red points). We observe that the THz emission from the nanostructured samples is enhanced compared to the emission from the flat samples when the azimuthal angle is 0°, which is also the configuration where plasmons are excited. The maximum enhancement occurs when the period of the sample is near to 230 nm. From Figure 3a we see that, at this grating period, the plasmon resonance occurs around 800 nm, the center wavelength of the incident femtosecond laser pulses. This provides strong evidence that plasmon excitation results in enhanced THz emission from the Au/Cu_2O thin films. The measured THz emission from samples having an oxide thickness of ∼232 nm, is also shown in Figure 6b. Once again, the maximum terahertz emission from the nanostructured samples occurs when the grating period is close to 230 nm. Maximum terahertz emission is observed from a sample of grating period 230 nm, and Cu_2O thickness ∼232 nm, when the coherent optical absorption and the plasmon resonance are both close to the laser excitation wavelength. The THz emission from a sample with a grating period of 230 nm and a Cu_2O thickness of 232 nm was experimentally observed to be about 2 times higher in power, than that from a sample of the same period and thickness 166 nm.

AZIMUTHAL ANGLE DEPENDENCE

To further emphasize the importance of plasmon excitation in enhancing the THz emission, we plot in Figure 7 the measured pump power absorption and the THz emission of nanostructured Au/Cu_2O samples with $\Lambda = 280$ and 230 nm as a function of the azimuthal angle. The thickness of the Cu_2O layer on both samples was around 232 nm. Note that at this thickness there is a maximum at a wavelength of 800 nm in the thickness-dependent pump-power absorption due to coherent optical absorption. The percentage of the incident pump power absorbed by the samples is represented by the black points in

dx.doi.org/10.1021/ph500251a | ACS Photonics 2014, 1, 1165−1172

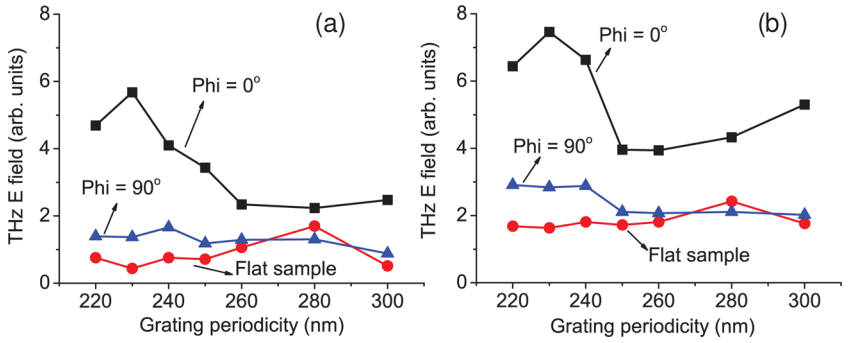

Figure 6. Electric field of the THz pulses emitted from the nanostructured samples, as a function of the grating period, for samples of Cu_2O thickness 166 nm (left) and 232 nm (right). The electric-field of the THz pulses emitted when the grating grooves are oriented perpendicular to the plane of incidence ($\phi = 0°$) of the pump beam is shown in black. In blue is the THz emission when the grating grooves are oriented parallel to the plane of incidence of the pump beam ($\phi = 90°$). The red points show the THz emission from the flat sample. In all cases, the incident light is p-polarized. The arbitrary units on the vertical axes are different for the two graphs and their amplitudes cannot be compared.

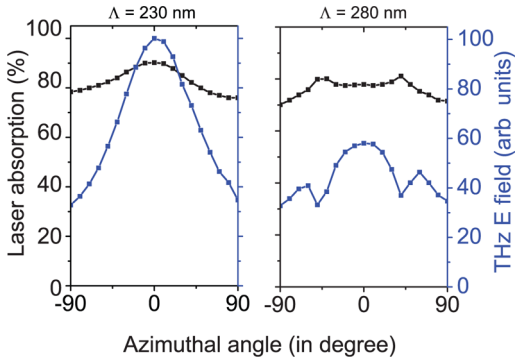

Figure 7. Azimuthal angle dependence of the electric-field strength of the emitted THz pulses (in blue) from two nanostructured Au/Cu_2O samples of period 230 nm (left) and 280 nm (right). Also shown is the corresponding pump power absorption expressed as a percentage of the incident power (in black).

both graphs. The blue points show the peak-to-peak values of the electric field of the emitted THz pulses. The THz electric-field amplitude is normalized to the maximum value measured. When $\Lambda = 230$ nm, the grating period supports the excitation of surface plasmons at the Au/Cu_2O interface, at the incident laser wavelength. When the azimuthal angle is varied from $-90°$ to $0°$, the percentage of absorbed pump power increases from about 75% to 90%. However, for the same change in the azimuthal angle, the electric field strength of the emitted THz pulses increases by a factor of ~3 (shown as the blue line), corresponding to an increase in THz power by a factor of 9. This is a much more dramatic increase compared to the increase in the absorbed pump power.

When $\Lambda = 280$ nm, the pump power absorption shows a peak at $\phi = \sim 45°$. Surprisingly, this peak in the laser absorption is accompanied by a *reduction* in the emitted THz amplitude. We observe a similar behavior for the samples with a Cu_2O film thickness of ~166 nm and $\Lambda = 280$ nm, which is shown in the Supporting Information, Figure S4. These peaks in the absorption also correspond to the dips observed in the reflection spectra of these samples, as discussed in the next section.

Figure 8a,b shows the measured normalized reflected intensity of the nanostructured Au/Cu_2O thin films with $\Lambda = 230$ and 280 nm, respectively, as a function of the azimuthal angle and as a function of wavelength. The thickness of the Cu_2O layer is ~232 nm in both cases and the incident light is p-polarized. The color bar indicates the reflected intensity, normalized to the reflection from a bare Au surface.

The coherent optical absorption, which depends on the thickness of the Cu_2O layer, occurs for both $\Lambda = 230$ and 280 nm samples at a wavelength a little above our wavelength of interest of 800 nm and is marked as "E". A plasmon resonance labeled "−1" is observed at a wavelength close to 800 nm for the sample with $\Lambda = 230$ nm, at $\phi = 0°$ (Figure 8a). The plasmon resonances depend on the azimuthal angle and disappears when ϕ increases to 90 deg, as expected, leaving only the coherent optical absorption which occurs at almost the same wavelength. For the sample with $\Lambda = 280$ nm (Figure 8b), the plasmon resonance is observed at a wavelength of 975 nm at $\phi = 0°$. It corresponds to $N = -1$ and is marked as −1 in the figure. In Figure 8b the plasmon resonance corresponding to $N = +1$ is also visible at a wavelength of 730 nm, at $\phi = 0°$. This is marked in the figure as +1 (see also Figure 4).

Numerical simulations are performed using an in-house developed software called "Cyclops" for solving Maxwell's equations.[19,20] The software is based on the finite element method described in the paper by Lalanne et al.[21] (called FEM1 in that article), which was tested and benchmarked against other methods such as the finite-difference time domain method. 2D simulations were performed for wavelengths ranging from 600 to 1000 nm. The angle of incidence was set to be 45° and the azimuthal angle was varied from 0° to 90°. A quadrilateral mesh was used such that for every material we had several mesh points per wavelength. The convergence of the simulations was verified by using a finer mesh, which did not change the results we obtained. Using the simulations, we calculated the reflected intensity in the far-field, and the electric and magnetic near-field spatial distributions at the grating, which enabled us to plot cross sections of the light intensity at the grating. Refractive indices of different, flat Cu_2O and AuCu thin films, measured using ellipsometry, were used in the simulation of the nanostructured sample. In order to have a better match with the measured plasmon resonance wavelength, the real part of the frequency-dependent refractive index of the Cu_2O film obtained from the flat sample has to be decreased by 7% in the case of the nanostructured sample. The thickness of the oxide was then adjusted accordingly from 166 and 232 nm to 171 and 250 nm, respectively, so that the etalon resonance wavelength does not change. Through the simulations we calculated the reflected electric field at the far-field (Figure 8). The simulated reflection spectra of the samples

dx.doi.org/10.1021/ph500251a | ACS Photonics 2014, 1, 1165−1172

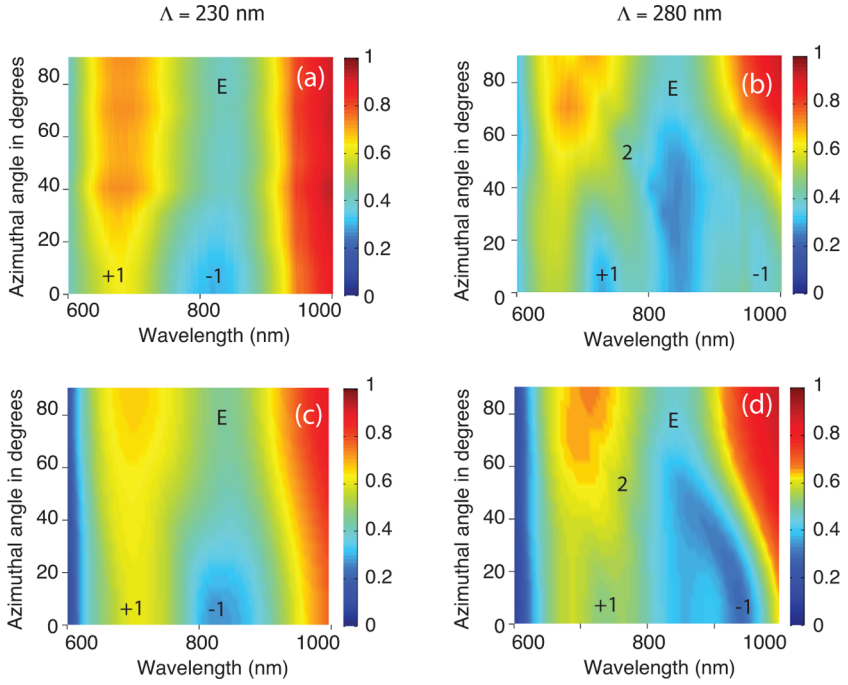

Figure 8. White-light reflection spectra of the nanostructured Au/Cu_2O samples as a function of the azimuthal angle. The incident light is p-polarized, and the angle of incidence is 45°. (a, b) Measured reflection spectra from the nanostructured samples of period 230 and 280 nm, respectively, for samples with Cu_2O thickness around 232 nm, and (c, d) corresponding simulated reflection spectra.

with an oxide thickness of 250 nm (corresponding to 232 nm in the measurement) and a grating period of 230 and 280 nm are shown in Figure 8c and d, respectively. The simulated spectra show a good agreement with the measured spectra. It was observed from the calculations that the strength of the plasmon resonances depends critically on the etch depth of the grating. The etch depth was assumed to be 17 nm in the simulations, which provided a better match with the experimentally measured reflection spectra. However, the measured Si etch depth is around 50 nm, and the discrepancy is assumed to arise from the incomplete oxidation of Cu within the trenches, giving rise to a smaller effective etch depth.

In Figure 8b, in addition to the plasmon and etalon dips in the reflection spectra, we can also see the presence of another resonance which appears as a diagonal line (marked 2). For clarity, the reflection spectra at three different azimuthal angles, 40, 60, and 80°, are shown in Figure 9. The arrows point to the extra dip observed in the reflection spectra. The wavelength at which this resonance occurs is a function of the azimuthal angle

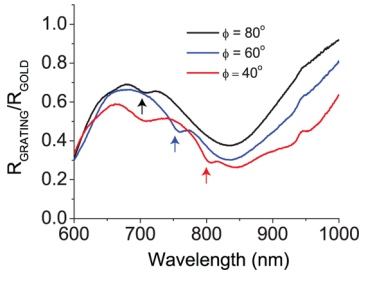

Figure 9. Measured white-light reflection spectra from the nanostructured Au/Cu_2O interfaces, with a grating periodicity of 280 nm and a Cu_2O thickness ~232 nm are shown for different azimuthal angles. The dips in the reflection spectra that are marked with arrows are responsible for the diagonal feature marked as "2" in Figure 8b.

and the thickness of the Cu_2O layer. We can see that this extra resonance occurs at a wavelength of 750 nm at ϕ = 60° and moves to a wavelength of 800 nm at ϕ = 40°. These azimuthal angles are close to the values at which we observe an absorption peak in the pump laser absorption and, simultaneously, a dip in the emitted THz amplitude in Figure 7. We stress that this resonance is not related to plasmon excitation. We speculate that this dip in the reflection spectra corresponds to a waveguide mode in the oxide thin film. The maximum pump electric field in such a mode is typically not reached at the metal surface but some distance away from it, and this decreases the efficiency of THz generation.

The measurements and calculations have so far provided strong evidence that plasmon excitation is responsible for the enhanced THz emission from nanostructrued Cu_2O/Au interfaces. To shed more light on the role played by surface plasmons, we also simulated the electric near field spatial distribution, to determine what the local pump fields look like when plasmons are excited. In Figure 10, we plot the *calculated* distributions of the near-field $|E(x,z,\lambda)|^2$ intensity of the pump light of wavelength 800 nm on the samples of oxide thickness 166 nm (171 nm in calculations) and 232 nm (250 nm in calculations). Here, $E(x,z,\lambda)$ is the position-dependent and wavelength-dependent total electric-field amplitude. For each thickness of the oxide layer (171 and 250 nm), two cases are shown, corresponding to azimuthal angles of 0° and 90°. The 800 nm light is incident at an angle of 45° from the top-left side of the figure. At ϕ = 0°, we observe plasmon-like modes for both 171 and 250 nm thick Cu_2O samples. There is a strong electric field at the interface of AuCu and Cu_2O, which is vertically well-confined, characteristic of surface plasmon polariton modes. At ϕ = 90°, there is very little field inside the Cu_2O thin film, and no features associated with plasmon excitation are seen. Compared to the sample with an oxide thickness of 250 nm, the sample with a 171 nm thick oxide film

dx.doi.org/10.1021/ph500251a | ACS Photonics 2014, 1, 1165−1172

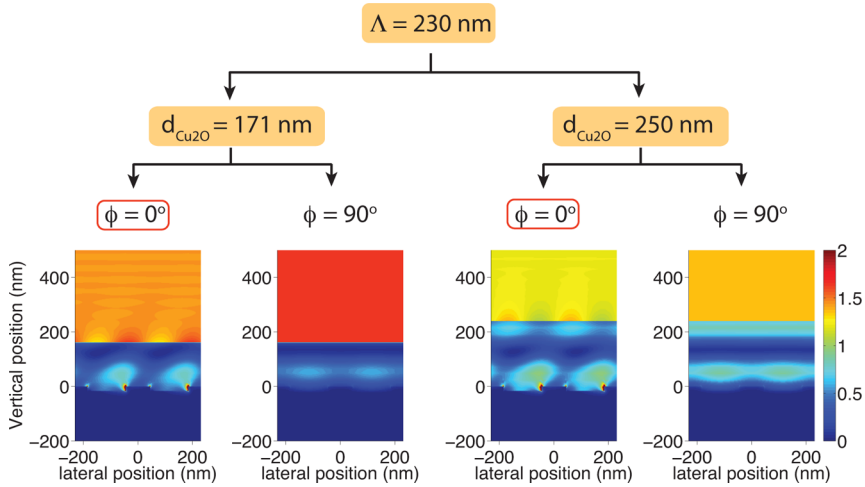

Figure 10. Simulated optical near-field cross sections of nanostructured Au/Cu_2O thin films, with a grating period of 230 nm, and thicknesses of 171 and 250 nm, at azimuthal angles of 0° and 90°. The plotted quantity is $|E(x,z,\lambda)|^2$. The wavelength of the incident light is 800 nm in the simulations. The cases where plasmon excitation is expected are denoted by the red box around the value of the azimuthal angle.

has more light reflected from the sample, due to constructive interference in the reflected direction. The red box surrounding the azimuthal angle values in the figure denotes that plasmon excitation is expected in this case.

CONCLUSION

From the experiments and simulations, we conclude that both optical absorption and THz emission from Au/Cu_2O layers occur in a region near the Schottky interface, where the static electric field has a maximum. Hence, for increasing the THz emission, it is important that the absorption of the laser light takes place near the interface. We have shown that, by nanostructuring the interfaces between Au and Cu_2O, we can excite surface plasmons, which localize pump laser energy at the interface. The evidence for surface-plasmon-enhanced THz emission can be summarized as follows:

The strongest THz emission was obtained from a sample of grating period 230 nm. We have seen from the white-light reflection spectra that the plasmon resonances depend on the grating period, and that a period of 230 nm is suitable for excitation of surface plasmons at 800 nm wavelength, as predicted. From the azimuthal angle-dependence measurements we see that the maximum pump power absorption and THz emission occur when the grating is oriented vertically and the incident laser is p-polarized. This orientation is optimal for the excitation of the surface plasmons. These measurements also indicate that concentrating the absorption of the pump laser light at the interface leads to an increase in the efficiency of THz emission. In other words, it is not just the absorption of the laser by the sample that is important, but where it is absorbed. This is also seen from the azimuthal angle dependence of THz emission from the sample of period 280 nm, where a peak in the absorption is observed at an azimuthal angle of 45°. However, this does not result in an increased THz emission, but on the contrary, in a decreased THz emission. One reason for this decrease in the THz emission is that a resonant mode is excited, presumably a waveguide mode for which the pump light is concentrated away from the interface, thus, contributing less to THz emission. Thus, the measurements and calculations clearly show that to maximize THz emission it matters more where the light is absorbed than how much is absorbed. This understanding may lead to new and improved THz emitters.

ASSOCIATED CONTENT

Supporting Information

(1) Sample fabrication, (2) Reflection spectra when the azimuthal angle is 90°, (3) Experimental setup for THz generation and detection, (4) Azimuthal angle dependence of THz emission for oxide thickness of 166 nm, and (5) Magnetic near field simulations. This material is available free of charge via the Internet at http://pubs.acs.org.

AUTHOR INFORMATION

Corresponding Author

*E-mail: g.r.kottayipilappara@tudelft.nl. Phone: +31 (0)15 27 81444. Fax: +31 (0)15 27 88105.

Notes

The authors declare no competing financial interest.

ACKNOWLEDGMENTS

P.C.M.P. and A.J.L.A. gratefully acknowledge the financial support from the Nederlandse Organisatie voor Wetenschappelijk Onderzoek (NWO) and the Stichting voor Technische Wetenschappen (STW) in the form of VICI and VENI Grants, respectively.

REFERENCES

(1) Pickwell, E.; Wallace, V. Biomedical applications of terahertz technology. *J. Phys. D: Appl. Phys.* **2006**, *39*, R301−R310.

(2) Tonouchi, M. Cutting-edge terahertz technology. *Nat. Photonics* **2007**, *1*, 97−105.

(3) Bonvalet, A.; Joffre, M.; Martin, J. L.; Migus, A. Generation of ultrabroadband femtosecond pulses in the mid-infrared by optical rectification of 15 fs light pulses at 100 MHz repetition rate. *Appl. Phys. Lett.* **1995**, *67*, 2907−2909.

(4) Graf, S.; Sigg, H.; Bächtold, W. High-frequency electrical pulse generation using optical rectification in bulk GaAs. *Appl. Phys. Lett.* **2000**, *76*, 2647−2649.

(5) Krokel, D.; Grischkowsky, D.; Ketchen, M. B. Subpicosecond electrical pulse generation using photoconductive switches with long carrier lifetimes. *Appl. Phys. Lett.* **1989**, *54*, 1046−1047.

(6) Jepsen, P.; Jacobsen, R.; Keiding, S. Generation and detection of terahertz pulses from biased semiconductor antennas. *J. Opt. Soc. Am. B* **1996**, *13*, 2424−2436.
(7) Berry, C. W.; Jarrahi, M. Terahertz generation using plasmonic photoconductive gratings. *New J. Phys.* **2012**, *14*, 105029.
(8) Que, C. T.; Edamura, T.; Nakajima, M.; Tani, M.; Hangyo, M. Terahertz Radiation from InAs Films on Silicon Substrates Excited by Femtosecond Laser Pulses. *Jpn. J. Appl. Phys.* **2009**, *48*, 010211.
(9) Jin, Y.; Ma, X. F.; Wagoner, G. A.; Alexander, M.; Zhang, X. C. Anomalous optically generated THz beams from metal/GaAs interfaces. *Appl. Phys. Lett.* **1994**, *65*, 682−684.
(10) Zhang, X.-C.; Darrow, J. T.; Hu, B. B.; Auston, D. H.; Schmidt, M. T.; Tham, P.; Yang, E. S. Optically induced electromagnetic radiation from semiconductor surfaces. *Appl. Phys. Lett.* **1990**, *56*, 2228−2230.
(11) McBryde, D.; Gow, P.; Berry, S. A.; Barnes, M. E.; Aghajani, A.; Apostolopoulos, V. Multiple double-metal bias-free terahertz emitters. *Appl. Phys. Lett.* **2014**, *104*.
(12) Protemics GmbH. http://protemics.com/index.php/products/thz-emitters/54-terablast.
(13) Ramakrishnan, G.; Ramanandan, G. K. P.; Adam, A. J. L.; Xu, M.; Kumar, N.; Hendrikx, R. W. A.; Planken, P. C. M. Enhanced terahertz emission by coherent optical absorption in ultrathin semiconductor films on metals. *Opt. Express* **2013**, *21*, 16784−16798.
(14) Kishino, K.; Unlu, M.; Chyi, J.-I.; Reed, J.; Arsenault, L.; Morkoc, H. Resonant cavity-enhanced (RCE) photodetectors. *IEEE J. Quantum Electron.* **1991**, *27*, 2025−2034.
(15) Raether, H. *Surface Plasmons on Smooth and Rough Surfaces and on Gratings*; Springer-Verlag: New York, 1988; Vol. *111*.
(16) Palik., E. D. *Handbook of Optical Constants of Solids*; Academic Press: Boston, 1985.
(17) Kats, M. A.; Blanchard, R.; Genevet, P.; Capasso, F. Nanometre optical coatings based on strong interference effects in highly absorbing media. *Nat. Mater.* **2013**, *12*, 1476−1122.
(18) Ramanandan, G. K. P.; Adam, A. J. L.; Ramakrishnan, G.; Petrik, P.; Hendrikx, R.; Planken, P. C. M. Optical characterization of gold-cuprous oxide interfaces for terahertz emission applications. *Appl. Opt.* **2014**, *53*.
(19) Wei, X.; Wachters, A. J.; Urbach, H. P. Finite-element model for three-dimensional optical scattering problems. *J. Opt. Soc. Am. A* **2007**, *24*, 866−881.
(20) Wei, X. Three dimensional rigorous model for optical scattering problems. Ph.D. Thesis, Delft University of Technology, 2006.
(21) Lalanne, P.; et al. Numerical analysis of a slit-groove diffraction problem. *J. Eur. Opt. Soc. Rapid Publ. A.* **2007**, *2*, 07022.